Upper critical field and its anisotropy in LiFeAs

J. L. Zhang,[1] L. Jiao,[1] F. F. Balakirev,[2] X. C. Wang,[3] C. Q. Jin,[3] and H. Q. Yuan[1,*]

[1]*Department of Physics, Zhejiang University, Hangzhou, Zhejiang 310027, China*

[2]*NHMFL, Los Alamos National Laboratory, MS E536, Los Alamos, New Mexico 87545, USA*

[3]*Beijing National Laboratory for Condensed Matter Physics, Institute of Physics, Chinese Academy of Science, Beijing 100080, China*

(Received 13 January 2011; revised manuscript received 16 March 2011; published 6 May 2011)

The upper critical field $\mu_0 H_{c2}(T_c)$ of LiFeAs single crystals has been determined by measuring the electrical resistivity using the facilities of pulsed magnetic field at Los Alamos. We found that $\mu_0 H_{c2}(T_c)$ of LiFeAs shows a moderate anisotropy among the layered iron-based superconductors; its anisotropic parameter γ monotonically decreases with decreasing temperature and approaches $\gamma \simeq 1.5$ as $T \to 0$. The upper critical field reaches 15 T ($H \parallel c$) and 24.2 T ($H \parallel ab$) at $T = 1.4$ K, which values are much smaller than those of other iron-based high T_c superconductors. The temperature dependence of $\mu_0 H_{c2}(T_c)$ can be described by the Werthamer-Helfand-Hohenberg (WHH) method, showing orbitally and (likely) spin-paramagnetically limited upper critical fields for $H \parallel c$ and $H \parallel ab$, respectively.

DOI: 10.1103/PhysRevB.83.174506 PACS number(s): 74.70.Xa, 71.35.Ji, 74.25.Op

I. INTRODUCTION

The discovery of superconductivity in iron pnictides[1] has attracted world-wide interest in searching for new types of high-T_c superconductors and unveiling their unconventional nature of superconductivity. Until now, several series of iron-based superconductors have been found[2] which possess a layered crystal structure similar to that of the high-T_c cuprates. Resembling the cuprates and heavy fermions, superconductivity in most of the iron pnictides/chalcogenides seems to be closely tied up with magnetism:[2] superconductivity appears while antiferromagnetism is suppressed by hole (or electron) doping or by application of external pressure. In particular, the layered crystal structure and the high superconducting transition temperatures of the iron pnictides/chalcogenides initially suggested a strong analogy with the cuprates, providing an alternative to study the puzzles of high-T_c superconductivity.

However, significant discrepancies have been observed between the iron-based superconductors and other layered superconductors. For example, d-wave superconductivity was realized in the high-T_c cuprates, but an $s\pm$-type order parameter has been proposed for the iron pnictides/chalcogenides superconductors.[3–5] Upper critical field is another important superconducting parameter. A large upper critical field has been identified in both iron pnictides/chalcogenides and the cuprates, but the former show a rather weak effect of anisotropy.[6–8] In particular, nearly isotropic upper critical field $\mu_0 H_{c2}(T_c)$ has been observed in the 122- and 11-type iron pnictides/chalcogenides,[6,7] remarkably different from any other layered superconductors.

LiFeAs, a much cleaner compound with a large ratio of room-temperature resistivity to residual resistivity (RRR $\sim$ 40), seems to be very unique among the iron pnictide superconductors.[9–11] Bearing a nearly identical structure of $(Fe_2As_2)^{2-}$ and also a similar electronic structure to other iron pnictides,[12] LiFeAs, however, shows simple metallic behavior prior to entering the superconducting state, lacking evidence of structural/magnetic transitions. Moreover, the stoichiometric compound LiFeAs becomes superconducting at ambient pressure and without introducing additional charge carriers via doping. Nevertheless, LiFeAs still demonstrates a relatively high T_c ($T_c \simeq 18$ K), being comparable with those iron pnictides/chalcogenides whose parent compounds undergo a magnetic/structural transition. Unfortunately, LiFeAs is extremely air sensitive and many of its superconducting properties remain mysterious because of the restrictions of accessible experimental methods.

In LiFeAs the extrapolation of $\mu_0 H_{c2}$ near T_c to zero temperature gives a rather large value of $\mu_0 H_{c2}(0)$ ($\sim$80 T).[11] In order to fully track the field dependence of superconductivity, a strong magnetic field is desired. Here we report the first resistivity measurement of LiFeAs in a pulsed magnetic field down to 1.4 K, from which the temperature–magnetic-field phase diagram is well established. The upper critical field $\mu_0 H_{c2}$ is determined to be 15 T and 24.2 T at $T = 1.4$ K for $H \parallel c$ and $H \parallel ab$, respectively. In comparison with other series of iron pnictide superconductors, the upper critical field shows a moderate anisotropic effect and its value of $\mu_0 H_{c2}(0)$ is largely reduced.

II. EXPERIMENTAL METHODS

High-quality single crystals of LiFeAs have been grown by a self-flux technique.[13] The precursor of Li_3As was synthesized from Li pieces and As chips that were sealed in a Nb tube under Ar atmosphere and then treated at 650 °C for 15 h in a sealed quartz tube. The Li_3As, Fe, and As powders were mixed using the following ratio: Li:Fe:As = 1:0.8:1. The powder mixture was then pressed into a pallet in an alumina oxide tube. To prevent the vaporized Li from attacking the quartz tube at high temperature, the sample pallet was subsequently sealed in a Nb tube and a quartz tube under vacuum. The sealed quartz tube was heated at 800 °C for 10 h before heating up to 1100 °C at which it was held for another 10 h. Finally, it was cooled down to 800 °C at a rate of 5 °C per hour. Crystals with a size up to 4 mm × 3 mm × 0.5 mm were obtained. The whole preparation work were carried out in a glove box protected with high purity Ar gas.

The obtained single crystals were characterized by x-ray diffraction with a Mac Science diffractometer, by the electrical resistivity and specific heat in a PPMS system (Quantum

Design), and by ac susceptibility measurements using the Oxford cryogenic system (Maglab-Exa-12) prior to transport measurements in a pulsed magnetic field at Los Alamos. Observations of very sharp peaks of (00*l*) in the x-ray diffraction patterns together with a sharp superconducting transition in all the physical properties mentioned above confirmed a high quality of our single crystals.[13] The elemental composition, checked by inductively coupled plasma (ICP) analysis with a total sample mass of more than 10 mg, is determined to be very close to the stoichiometric ratio of LiFeAs.

Electrical resistivity was measured using a typical four-contact method in pulsed fields of up to 40 T and at temperatures down to 1.4 K in a helium-4 cryostat. In order to minimize the inductive self-heating caused by the fast change of magnetic field, small crystals with typical sizes 2 mm × 0.5 mm × 0.1 mm were cleaved off along the *c*- direction from the as-grown samples. The thin samples were first glued on a piece of sapphire (rectangularlike) using GE (General Electric) varnish before mounting on the sample holder. We switched the orientation of the magnetic field by mounting the sapphire slice in different directions. Note that the applied electrical current was always along the *ab* plane. In order to avoid oxidizing the samples, special care was paid to protect the samples from exposure to air while making the electrical contacts. Data were recorded using a 10-MHz digitizer and 100-kHz alternating current and analyzed using a custom low-noise digital lock-in technique. The temperature dependence of the electrical resistivity at zero field was measured with a Lakeshore resistance bridge.

III. EXPERIMENTAL RESULTS AND DISCUSSIONS

Figure 1 presents the temperature dependence of the electrical resistivity $\rho(T)$ at zero magnetic field for LiFeAs. Obviously, LiFeAs shows simple metallic behavior upon cooling down from room temperature, followed by a sharp superconducting transition at $T_c^{\rm mid} \simeq 17.5$ K. Note that the weak kink in the resistivity $\rho(T)$ around 75 K is attributed to the change of cooling rate. No evidence of structural/magnetic transition has been observed in LiFeAs. In order to demonstrate the superconducting transition in detail, we plot the low-temperature electrical resistivity and magnetic susceptibility in the inset of Fig. 1, which were measured with samples cut from the same batch. As frequently observed in superconductors, the bulk T_c ($T_c^{\rm onset} \simeq 17$ K and $T_c^{\rm mid} \simeq 15$ K) determined from the magnetic susceptibility is slightly lower than the resistive T_c ($\simeq$17.5 K). Note that the T_c values of our samples are compatible with those reported in the literature.[9–11] The observations of a large RRR ($\rho_0 \simeq 0.04$ mΩcm and RRR $\simeq 24$) and a narrow superconducting transition again indicate a high quality of the samples investigated here.

Since LiFeAs is a good metal with low resistivity, measurement of its electrical resistivity in a pulsed magnetic field is rather challenging. Nevertheless, we have succeeded in obtaining a good set of resistivity data up to a magnetic field of 40 T after many failures. Figure 2 shows the field dependence of the electrical resistivity $\rho(\mu_0 H)$ of LiFeAs at variant temperatures, in which the magnetic field is applied along (a) the *c* axis and (b) the *ab* plane, respectively. One can see that a relatively sharp superconducting transition survives down to very low temperatures, even though the signals become more noisy upon cooling down, in

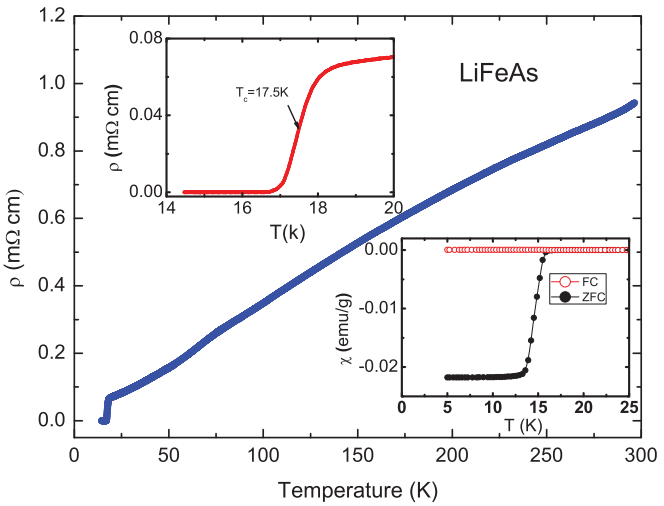

FIG. 1. (Color online) Temperature dependence of the electrical resistivity $\rho(T)$ for LiFeAs at zero field. The lower inset shows the magnetic susceptibility $\chi(T)$.

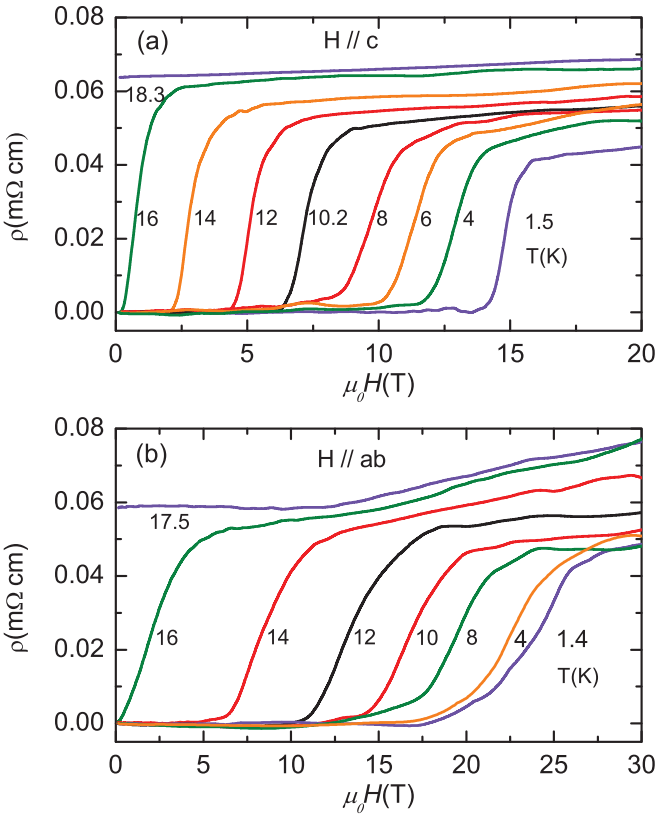

FIG. 2. (Color online) Magnetic field dependence of the electrical resistivity at variant temperatures for LiFeAs: (a) $H \parallel c$; (b) $H \parallel ab$.

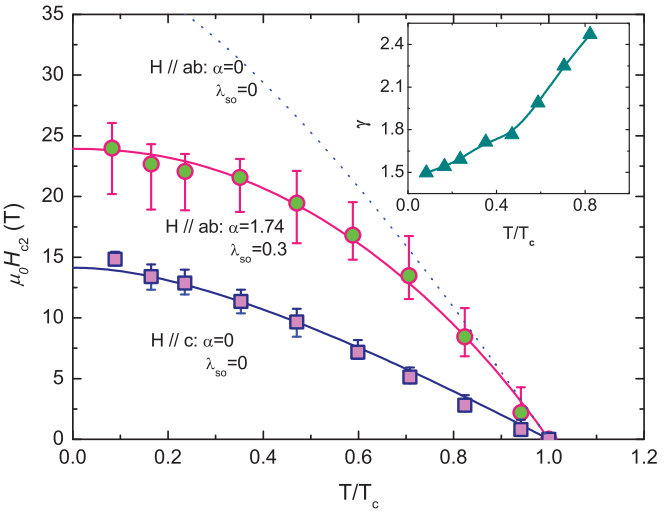

FIG. 3. (Color online) The upper critical field $\mu_0 H_{c2}(T_c)$ and the corresponding WHH fits for LiFeAs. The solid lines are the best fits to the experimental data and the dotted line is the WHH fit without considering the spin paramagnetic effect. The inset shows the temperature dependence of the anisotropic parameter γ.

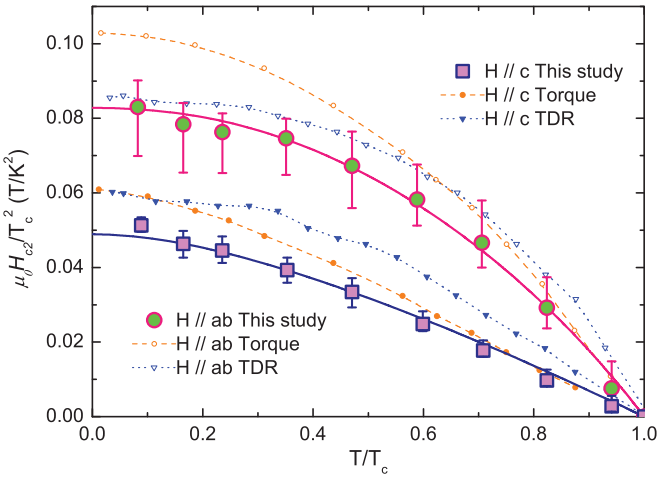

FIG. 4. (Color online) The scaled upper critical field $\mu_0 H_{c2}(T_c)/T_c^2$ versus the normalized temperature T/T_c for LiFeAs. Symbols of the square (□), circle (○), and triangle (∇) represent the data obtained from measurements of the electrical resistivity (this study), the magnetic torque,[24] and the resonant frequencies based on the tunnel-diode resonator (TDR),[25] respectively.

particular for the case of $H \parallel ab$. Obviously, the superconducting transition is eventually suppressed upon applying a magnetic field, but the critical field required to suppress superconductivity is much larger for $H \parallel ab$. Furthermore, the normal state of LiFeAs remains metallic upon suppressing superconductivity in a sufficiently high magnetic field, being different from that of some 122- and 11-type (underdoped) compounds.[6,7]

The upper critical field $\mu_0 H_{c2}(T_c)$ of LiFeAs, determined from the midpoint of the superconducting transition, is plotted in Fig. 3. The error bars were derived from the 20% and 80% drop of the normal state resistivity at T_c. In comparison with other families of the iron-based high-temperature superconductors,[6–8] LiFeAs shows a relatively small upper critical field, reaching $\mu_0 H_{c2} = 15$ T and 24.2 T at $T = 1.4$ K for $H \parallel c$ and $H \parallel ab$, respectively. Temperature dependence of the anisotropic parameter, defined as $\gamma = H_{c2}^{H\parallel ab}/H_{c2}^{H\parallel c}$, is plotted in the inset of Fig. 3. Resembling those of the previously investigated iron-based superconductors,[6–8] the anisotropic parameter γ decreases with decreasing temperature, reaching $\gamma = 1.5$ at zero temperature. Such a value of γ is slightly higher than that of the 122- and 11-type compounds,[6,7] which show nearly isotropic behavior at low temperatures, but is significantly smaller compared to that of the high-T_c cuprates and organic superconductors.[14,15]

According to the Werthamer-Helfand-Hohenberg theory,[16] the upper critical field limited by the orbital mechanisms in the dirty limit is given by

$$\mu_0 H_{c2}^{\rm orb}(0)[\mathrm{T}] = -0.69 T_c (dH_{c2}/dT)\,|_{T=T_c}[\mathrm{K}]. \qquad (1)$$

On the other hand, superconductivity is suppressed while the magnetic energy associated with the Pauli spin susceptibility in the normal state exceeds the condensation energy in the superconducting state as a result of Zeeman effect. In this case, the Pauli-limited upper critical field is usually defined by[17,18]

$$\mu_0 H_{c2}^{p}(0)[\mathrm{T}] = \Delta/\sqrt{2}\mu_B = 1.86 T_c[\mathrm{K}] \ \text{(for BCS SC)}, \qquad (2)$$

where Δ is the superconducting energy gap and μ_B is the Bohr magneton. The later expression in Eq. (2) is for conventional BCS superconductors.

The derived superconducting parameters are summarized in Table I for LiFeAs. For conventional superconductors, $\mu_0 H_{c2}^{p}(0)$ is usually much larger than $\mu_0 H_{c2}^{\rm orb}(0)$ and, therefore, their upper critical field is mainly restricted by the orbital pair-breaking mechanism. In our case, the initial slope of $\mu_0 H_{c2}$ at T_c, i.e., $-d(\mu_0 H_{c2})/dT|_{T=T_c}$, is determined as 3.3 T/K and 1.2 T/K for $H \parallel ab$ and $H \parallel c$, respectively. Thus the values of $\mu_0 H_{c2}^{\rm orb}(0)$ are accordingly derived as 39.8 T for $H \parallel ab$ and 14.5 T for $H \parallel c$; the latter is close to the experimental

TABLE I. The derived superconducting parameters for LiFeAs.

Field	T_c (K)	$-\frac{d\mu_0 H_{c2}}{dT}\big\vert_{T_c}$ (T/K)	$\mu_0 H_{c2}$ (1.4 K) (T)	$\mu_0 H_{c2}^{\rm orb}$ (T)	$\mu_0 H_{c2}^{p}$ (T)	α	λ_{so}	ξ (nm)
$H \parallel c$	17.5	1.2	15	14.5	32.6	0	0	1.7
$H \parallel ab$	17.5	3.3	24.2	39.8	32.6	1.74	0.3	4.8

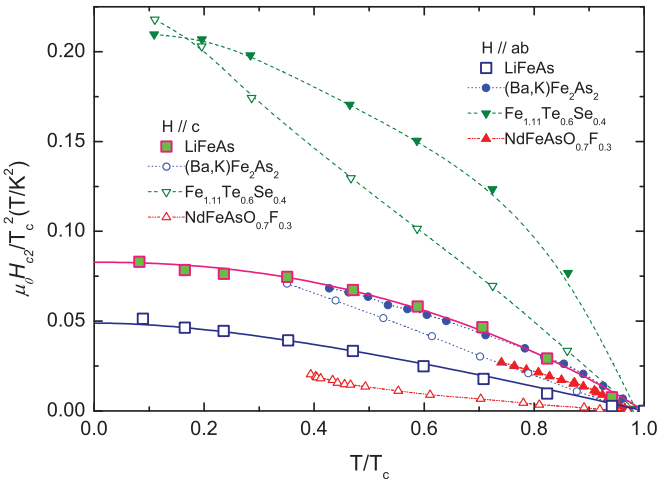

FIG. 5. (Color online) The upper critical field $\mu_0 H_{c2}/T_c^2$ versus the normalized temperature T/T_c for single crystals of LiFeAs (this study), (Ba,K)Fe_2As_2 (Ref. 6), $Fe_{1.11}Te_{0.6}Se_{0.4}$ (Ref. 7), and $NdFeAsO_{0.7}F_{0.3}$ (Ref. 8), in which $T_c = 17.5$, 55, 28, and 14 K, respectively. Note that variant symbols represent variant compounds as marked in the figure.

value of $\mu_0 H_{c2} \simeq 15$ T at $T = 1.4$ K, indicating an orbitally limited critical field for $H \parallel c$. On the other hand, Eq. (2) yields $\mu_0 H_{c2}^p(0) = 32.6$T. The experimentally derived value of $\mu_0 H_{c2}(0) \sim 25$T for $H \parallel ab$ is, therefore, well below the corresponding values of $\mu_0 H_{c2}^{\rm orb}(0)$ and $\mu_0 H_{c2}^p(0)$. The solid lines in Fig. 3 present the Werthamer-Helfand-Hohenberg (WHH) fits to the experimental data of $\mu_0 H_{c2}(T_c)$ following the methods given in Ref. 16, in which both the spin-paramagnetic and orbital pair-breaking effects were considered. The fitting parameters of α (the Maki parameter) and $\lambda_{\rm so}$ are defined by $\alpha = \sqrt{2} H_{c2}^{\rm orb}/H_{c2}^p$ and $\lambda_{\rm so} = 1/3\pi T_c \tau_2$, where τ_2^{-1} reflects the spin-orbit scattering rate.[16] The fits give the Maki parameter $\alpha = 0$ and 1.74 for the field along the c axis and the ab plane, respectively. The former further confirms the orbitally limited critical field for $H \parallel c$. However, the resulting parameters ($\alpha = 1.74, \lambda_{\rm so} = 0.3$) indicate that the upper critical field is likely spin-paramagnetically limited for $H \parallel ab$ even though we cannot fully exclude the orbital effect due to the complex nature of the interband scattering in this multiband superconductor.[19–23] As shown in Fig. 3 (see the dotted line and the solid line for $H \parallel ab$), the spin-paramagnetic effect might lower the upper critical field and, therefore, reduce the anisotropy of $\mu_0 H_{c2}$ at low temperatures.

For comparison, Fig. 4 plots the reported upper critical fields for LiFeAs, independently determined from measurements of the electrical resistivity (this work), the magnetic torque,[24] and the resonant frequencies based on a tunnel-diode oscillator.[25] One can see that the experimental results obtained from the above three methods are similar in general; the visible discrepancy might result from the detailed methods of determining T_c as well as a slight variation of the Li stoichiometry in LiFeAs. For example, T_c is determined from the midpoint of the resistivity drop at T_c in this study, but was determined from the superconducting onset in the measurements of magnetic torque (bulk properties)[24] and the TDR frequency shift (surface sensitive),[25] which may cause some deviations of T_c. On the other hand, the slight difference of T_c (about 2K) reported in these three experiments might indicate a small variation of the Li stoichiometry, leading to possible changes on $\mu_o H_{c2}(T_c)$ too. Nevertheless, all these experiments show similar results and the electrical resistivity studied here provides an alternative but more direct approach for determining the upper critical field.

In Fig. 5, we compare the upper critical field and its anisotropy in several typical iron-based superconductors, i.e., LiFeAs (this work), (Ba,K)Fe_2As_2 (Ref. 6), $Fe_{1.11}Te_{0.6}Se_{0.4}$ (Ref. 7), and $NdFeAsO_{0.7}F_{0.3}$ (Ref. 8). In general, the upper critical fields of all these compounds show a rather weak anisotropy at low temperatures in comparison with other layered superconductors, e.g., the high-T_c cuprates and the organic superconductors.[14,15] This indicates that the interlayer coupling might become significantly important in the iron-based superconductors, which was largely neglected for high-T_c cuprates. Among the iron-based superconductors, LiFeAs shows a relatively small upper critical field. For example, $Fe_{1.11}Te_{0.6}Se_{0.4}$ undergoes a superconducting transition at $T_c \simeq 14$ K, but it shows a much larger upper critical field [$\mu_0 H_{c2}(0) \simeq 45$ T], which is likely attributed to its higher disorder. In (Ba,K)Fe_2As_2 and $Fe_{1.11}Te_{0.6}Se_{0.4}$,[6,7] we observed nearly isotropic behavior of the upper critical field at low temperatures; this unique feature was attributed to the three-dimensional-like Fermi surface as experimentally confirmed later.[26] The moderate anisotropy of $\mu_0 H_{c2}$ in LiFeAs and the 1111 series is actually consistent with the band structure calculations which indicate an enhanced anisotropy in these systems.[12]

IV. CONCLUSION

In summary, we have determined the complete temperature–magnetic-field phase diagram for the superconductor LiFeAs by means of measuring the electrical resistivity in a field up to 40 T. The upper critical field of LiFeAs is derived as $\mu_0 H_{c2}(1.4\,{\rm K}) = 15$ T and 24.2 T for field applied along the c axis and the ab plane, respectively. The anisotropic parameter γ decreases with decreasing temperature and shows a weak anisotropic effect at low temperatures. These findings indicate that weak anisotropy of $\mu_0 H_{c2}$ seems to be a common feature of the iron-based superconductors, despite the layered nature of their crystal structure.

ACKNOWLEDGMENTS

This work was supported by the National Science Foundation of China, the National Basic Research Program of China (973 Program), the PCSIRT of the Ministry of Education of China, Zhejiang Provincial Natural Science Foundation of China, and the Fundamental Research Funds for the Central Universities. Work at NHMFL-LANL was performed under the auspices of the National Science Foundation, the Department of Energy, and the State of Florida.

*hqyuan@zju.edu.cn

[1] Y. Kamihara, T. Watanabe, M. Hirano, and H. Hosono, J. Am. Chem. Soc. **130**, 3296 (2008).

[2] See, e.g., Z. A. Ren and Z. X. Zhao, Adv. Mater. **21**, 4584 (2009); M. D. Lumsden and A. D. Christianson, J. Phys. Condens. Matter **22**, 203203 (2010).

[3] K. Seo, B. A. Bernevig, and J. P. Hu, Phys. Rev. Lett. **101**, 206404 (2008).

[4] I. I. Mazin, D. J. Singh, M. D. Johannes, and M. H. Du, Phys. Rev. Lett. **101**, 057003 (2008).

[5] T. Hanaguri, S. Niitaka, K. Kuroki, and H. Takagi, Science **328**, 474 (2010).

[6] H. Q. Yuan, J. Singleton, F. F. Balakirev, S. A. Baily, G. F. Chen, J. L. Luo, and N. L. Wang, Nature (London) **457**, 565 (2009).

[7] M. H. Fang, J. H. Yang, F. F. Balakirev, Y. Kohama, J. Singleton, B. Qian, Z. Q. Mao, H. D. Wang, and H. Q. Yuan, Phys. Rev. B **81**, 020509 (2010).

[8] J. Jaroszynski, F. Hunte, L. Balicas, Y. J. Jo, I. Raicevic, A. Gurevich, D. C. Larbalestier, F. F. Balakirev, L. Fang, P. Cheng, Y. Jia, and H. H. Wen, Phys. Rev. B **78**, 174523 (2008).

[9] X. C. Wang, Q. Q. Liu, Y. X. Lv, W. B. Gao, L. X. Yang, R. C. Yu, F. Y. Li, and C. Q. Jin, Solid State Commun. **148**, 538 (2008).

[10] J. H. Tapp, Z. Tang, B. Lv, K. Sasmal, B. Lorenz, P. C. W. Chu, and A. M. Guloy, Phys. Rev. B **78**, 060505 (2008).

[11] Y. J. Song, J. S. Ghim, B. H. Min, Y. S. Kwon, H. M. Jung, and J.-S. Rhyee, Appl. Phys. Lett. **96**, 212508 (2010).

[12] I. A. Nekrasov, Z. V. Pchelkina, and M. V. Sadovskii, J. Exp. Theor. Phys. Lett. **88**, 543 (2008).

[13] X. C. Wang, Q. Q. Liu, Y. X. Lv, Z. Deng, K. Zhao, R. C. Yu, J. L. Zhu, and C. Q. Jin, Sci. China - Phys. Mech. Astron. **53**, 1199 (2010).

[14] J. R. Shrieffer and J. S. Brooks, *Handbook of High-Temperature Superconductivity* (Springer, New York, 2006).

[15] J. Singleton and C. Mielke, Contemp. Phys. **43**, 63 (2002).

[16] N. R. Werthamer, E. Helfand, and P. C. Hohenberg, Phys. Rev. **147**, 295 (1966).

[17] A. M. Clogston, Phys. Rev. Lett. **9**, 266 (1962).

[18] B. S. Chandrasekhar, J. Appl. Phys. Lett. **1**, 7 (1962).

[19] D. J. Singh, Phys. Rev. B **78**, 094511 (2008).

[20] H. Kim, M. A. Tanatar, Y. J. Song, Y. S. Kwon, and R. Prozorov, Phys. Rev. **83**, 100502(R) (2011).

[21] U. Stockert, M. Abdel-Hafiez, D. V. Evtushinsky, V. B. Zabolotnyy, A. U. B. Wolter, S. Wurmehl, I. Morozov, R. Klingeler, S. V. Borisenko, and B. Büchner, e-print arXiv:1011.4246.

[22] Y. J. Song, J. S. Ghim, J. H. Yoon, K. J. Lee, M. H. Jung, H. S. Ji, J. H. Shim, and Y. S. Kwon, e-print arXiv:1007.4906.

[23] Y. Imai, H. Takahashi, K. Kitagawa, K. Matsubayashi, N. Nakai, Y. Nagai, Y. Uwatoko, M. Machida, and A. Maeda, J. Phys. Soc. Jpn **80**, 013704 (2011).

[24] N. Kurita, K. Kitagama, K. Matsubayashi, A. Kismarahardja, E-S. Choi, J. S. Brooks, Y. Uwatoko, S. Uji, and T. Terashima, J. Phys. Soc. Jpn. **80**, 013706 (2011).

[25] K. Cho, H. Kim, M. A. Tanatar, Y. J. Song, Y. S. Kwon, W. A. Coniglio, C. C. Agosta, A. Gurevich, and R. Prozorov, Phys. Rev. B **83**, 060502(R) (2011).

[26] P. Vilmercati, A. Fedorov, I. Vobornik, U. Manju, G. Panaccione, A. Goldoni, A. S. Sefat, M. A. McGuire, B. C. Sales, R. Jin, D. Mandrus, D. J. Singh, and N. Mannella, Phys. Rev. B **79**, 220503 (2009).